

# PROCEEDINGS OF SPIE

[SPIDigitalLibrary.org/conference-proceedings-of-spie](https://SPIDigitalLibrary.org/conference-proceedings-of-spie)

## Diffuse correlation spectroscopy in the Fourier domain with holographic camera-based detection

James, Edward, Powell, Samuel

Edward James, Samuel Powell, "Diffuse correlation spectroscopy in the Fourier domain with holographic camera-based detection," Proc. SPIE 11239, Dynamics and Fluctuations in Biomedical Photonics XVII, 112390H (21 February 2020); doi: 10.1117/12.2545177

**SPIE.**

Event: SPIE BiOS, 2020, San Francisco, California, United States

# Diffuse correlation spectroscopy in the Fourier domain with holographic camera-based detection

Edward James<sup>a</sup> and Samuel Powell<sup>b</sup>

<sup>a</sup>Department of Medical Physics & Biomedical Engineering, University College London, London, WC1E 6BT, UK.

<sup>b</sup>Faculty of Engineering, The University of Nottingham, University Park, Nottingham, NG7 2RD, UK.

## ABSTRACT

We present a new approach to Diffuse Correlation Spectroscopy (DCS) which overcomes the limited light throughput of single mode photon counting techniques, and operates with continuous wave illumination without disturbance from ambient light. Heterodyne holographic detection allows parallel measurement of the power spectrum of a fluctuating electric field across thousands of modes, from which we may directly compute flow parameters using a novel Fourier domain DCS model. Our detection and modelling strategy are rigorously validated by modulating the Brownian and flow components of an optical tissue phantom, demonstrating absolute measurements of the Brownian diffusion coefficient in excellent agreement with conventional methods. We demonstrate the feasibility of *in vivo* measurement through the recovery of pulsatile flow rates measured in the human forearm.

**Keywords:** diffuse correlation spectroscopy, heterodyne holography, cerebral blood flow

## 1. INTRODUCTION

DCS is an optical imaging modality in which the ensemble average of flow within a tissue sample can be inferred from measurement of the intensity autocorrelation function of light that has passed through the sample. A general rule of thumb in diffuse optics is that a banana-shaped region of depth equal to one half to one third of the optical source-detector separation (SDS) distance is sampled.<sup>1,2</sup> Thus for a typical DCS setup with a SDS distance of 2-3 cm, only superficial cortical flow is sampled. To date, deep CBF has not been measured using DCS in human studies.<sup>1</sup>

Conventional implementations of DCS typically employ single mode photon counting techniques. Such methods are limited by low light throughput,<sup>1</sup> and by their sensitivity to ambient light.<sup>3</sup> Increasing penetration depth requires the use of larger SDS distances, which will decrease available SNR further by increasing the number of absorption and scattering events, since the attenuation of near-infrared (NIR) light by these two mechanisms is in the order of 10 dB/cm.<sup>4</sup> The low light level in a single speckle places a minimum limit on the detection time for single mode detection.<sup>5</sup>

Increasing acquisition time can resolve this situation but leads to a reduction in temporal resolution. Taking the average of many single-mode detection fibres bundled together is an expensive option that requires many photon counting detectors and can increase complexity of system integration. Improved collection optics, the use of few-mode detection fibres, and increasing the amount of light delivered to the tissue can also help to improve SNR. However, patient safety limits must be adhered to, which necessitates an optical source of sufficiently large diameter and low power rating. All of the above characteristics limit the applicability of DCS in portable continuous monitoring applications to which optical methods are otherwise well suited.

Previous authors have noted that improvements to increase SNR and temporal resolution will help the development of DCS functional experiments, as well as expand the range of uses for DCS in clinical monitoring.<sup>1</sup> The utility of high frame rate ( $\sim 20$  Hz) DCS measurements, compared to the frame rates of 0.3 to 1 Hz that have

---

Further author information: (Send correspondence to Edward James)  
Edward James: E-mail: e.james.14@ucl.ac.uk

Dynamics and Fluctuations in Biomedical Photonics XVII, edited by Valery V. Tuchin  
Martin J. Leahy, Ruikang K. Wang, Proc. of SPIE Vol. 11239, 112390H  
© 2020 SPIE · CCC code: 1605-7422/20/\$21 · doi: 10.1117/12.2545177

Proc. of SPIE Vol. 11239 112390H-1

historically been used, has also been discussed.<sup>6</sup> These benefits include improved monitoring of cerebrovascular autoregulation dynamics, more robust identification of motion artefacts, and increased measurement throughput that could enable high spatial resolution with fewer detectors.

Improvements in SNR are also motivated by the ability to perform flow measurements with improved spatial resolution and depth penetration through the use of acousto-optic tomography (AOT),<sup>5,7,8</sup> which is an emerging hybrid imaging modality that makes use of the ultrasound modulation of light.<sup>9</sup> The modulation efficiency of photons by ultrasound is low at biologically safe power levels, and therefore significantly improved SNR is required in order to detect this modulated component.

We present a high speed Fourier domain implementation of DCS suitable for making *in vivo* pulsatile flow measurements. Our approach employs a holographic parallel detection method known as heterodyne parallel speckle detection (HPSD), which averages over thousands of modes to realise improvements in SNR, and which operates with continuous wave illumination without disturbance from ambient light. Unlike conventional photon counting methods, this technique records the power spectral density of the light scattered and broadened by the sample. These measurements can then be fit to a novel Fourier domain DCS model, from which we directly compute flow parameters in real-time.

HPSD has been well described in the literature since its inception in 2003.<sup>10–13</sup> The experimental configuration consists of a Mach-Zender interferometer, where the reference and sample arms are combined and interfere on a digital camera. Temporal filtering occurs over the camera integration period, and the resulting images record the first-order power spectral density of the scattered electric field,  $S_1$ , at a particular frequency. By detuning the frequency of the reference arm of the interferometer by a pair of Bragg cells,  $S_1$  may be sampled at frequency shifts ( $\Delta f$ ) from that of the input optical field, allowing the frequency spectrum of the scattered light to be acquired. The heterodyne gain and shot noise limited performance<sup>12</sup> of this technique permit illumination below the maximum permissible exposure limits of tissue, and it is therefore particularly suited to *in vivo* flow detection.<sup>7</sup> HPSD has previously been used to measure convective flow rates *in vitro*, by fitting measured power spectra to a Fourier domain diffusing wave spectroscopy (DWS) model of convective motion.<sup>14</sup> This group quantified diffusive Brownian motion by fitting measured data to the discrete Fourier transform of a DWS model of Brownian motion. The same study also measured localised superficial microvascular convective flow rates in the cerebral cortices of 2 mice and the retinas of 3 adult rats. However, this study used a camera exposure time of 30 ms and a camera frame rate of 12 Hz, which provided insufficient temporal resolution to perform high frame rate pulsatile *in vivo* imaging, especially after frame averaging. Additionally, it is well documented in the DCS literature that a Brownian diffusion model, rather than a convective motion model, provides a better fit to measured DCS data over a broad range of tissue types.<sup>2,15</sup>

## 2. METHOD

Using HPSD to measure deep flow, at rates sufficient to resolve pulsatile information, brings significant challenges. To employ holographic DCS in a practical *in vivo* setting requires that we use short exposure times in order to minimise the effects of sample movement and external sources of vibration which disrupt the interferometric configuration. Additionally short exposure times are required to facilitate a high parameter output rate that can resolve fast pulsatile changes. However, reducing the exposure time comes at the cost of a wider instrument response function (IRF), which will result in a broadening of the measured power spectra, which in turn will increase the complexity of data sampling and interpretation.

The relatively slow exposure frame rates available through camera-based detection are not conducive to the fast parameter output rates that are required for high temporal resolution *in vivo* pulsatile detection. Compared to conventional DCS, data acquisition speed and processing load are high, especially if we wish to achieve real-time data acquisition at high parameter output rates. There is also a trade-off to consider between speed of data acquisition, making use of averaging to improve SNR, and sampling the measured power spectra at a sufficient number of frequency shifts so as to permit robust fitting to a forward model.

Whilst the true autocorrelation and power spectral density of the scattered light form a Fourier transform pair, the data measured using conventional and holographic DCS systems will deviate due to differences in the nature of the measurement systems. These differences arise due to the nature of the sampling in the two domains,

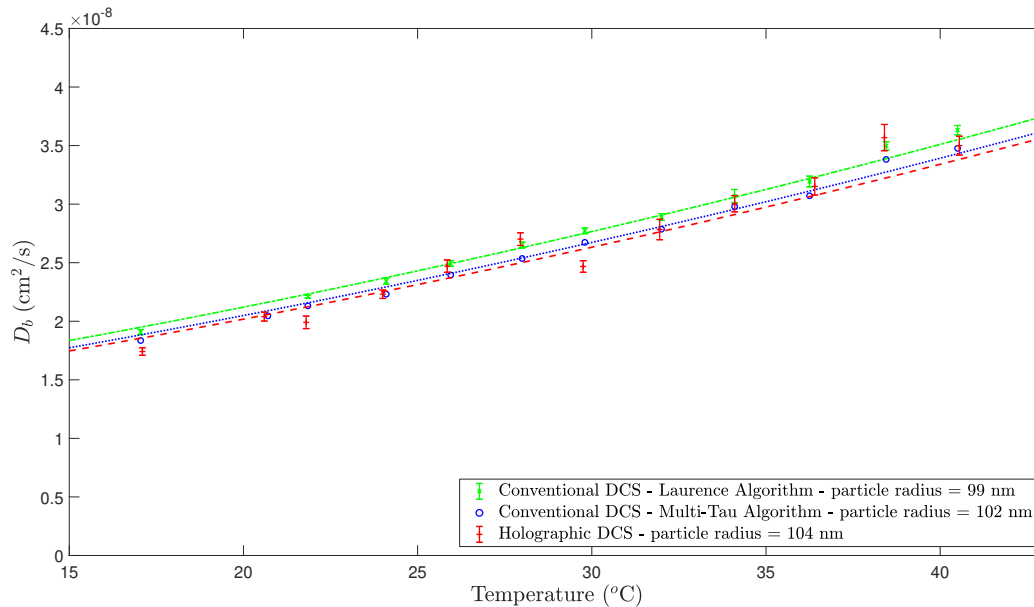


Figure 1. Fitting measured  $D_b$  data to the Stokes-Einstein equation over a temperature range in order to predict the particle radius within an intralipid tissue phantom.

the effects of IRF broadening and static scatterers, and the differing effects of measurement noise in the two configurations.

We have therefore developed a custom holographic DCS instrument with a high throughput that makes use of a highly parallel GPU-accelerated holographic demodulation pathway, which permits real-time measurement of the power spectral density of light scattered by a diffusing sample. For example, our instrument is capable of measuring the power spectral density of the electric field across  $\sim 1,110$  speckles at 6 discrete frequency shifts with an overall parameter output rate of 23.8 Hz. We have developed a novel Fourier domain Brownian DCS model, which allows for native domain fitting of holographic DCS data and flow parameter extraction. Knowledge of the IRF<sup>10</sup> of a holographic DCS instrument allows us to optimise both detection strategies and flow parameter fitting.

### 3. RESULTS

Validation of our holographic DCS instrument was achieved by computing the particle radii within an intralipid tissue phantom (Intralipid 20 %, Fresenius Kabi), as predicted by the Stokes-Einstein equation<sup>14,16-18</sup>

$$D_b = \frac{k_B T}{6\pi\eta r}, \quad (1)$$

where  $D_b$  is the Brownian diffusion coefficient,  $k_B$  is Boltzmann's constant,  $T$  is absolute temperature,  $\eta$  is dynamic viscosity, and  $r$  is the hydrodynamic radius of spherical particles diffusing through a liquid. The intralipid phantom was held at a range of temperatures using a thermostatically controlled waterbath, and  $D_b$  values acquired from conventional DCS (using both multi-tau<sup>15,19</sup> and Laurence<sup>20</sup> autocorrelation algorithms) and our holographic DCS instrument over this temperature range were used to optimise for particle radius (Figure 1). Transmission electron microscopy measurements of intralipid by the same manufacturer suggest a particle radius of 107 nm.<sup>21</sup> Our holographic DCS instrument produced the closest estimate to this ground-truth value (within 3 %). All three of the particle radii shown in Figure 1 are within a maximum 5 % deviation of each other, which validates the accuracy and interpretation of the data produced by our instrument.

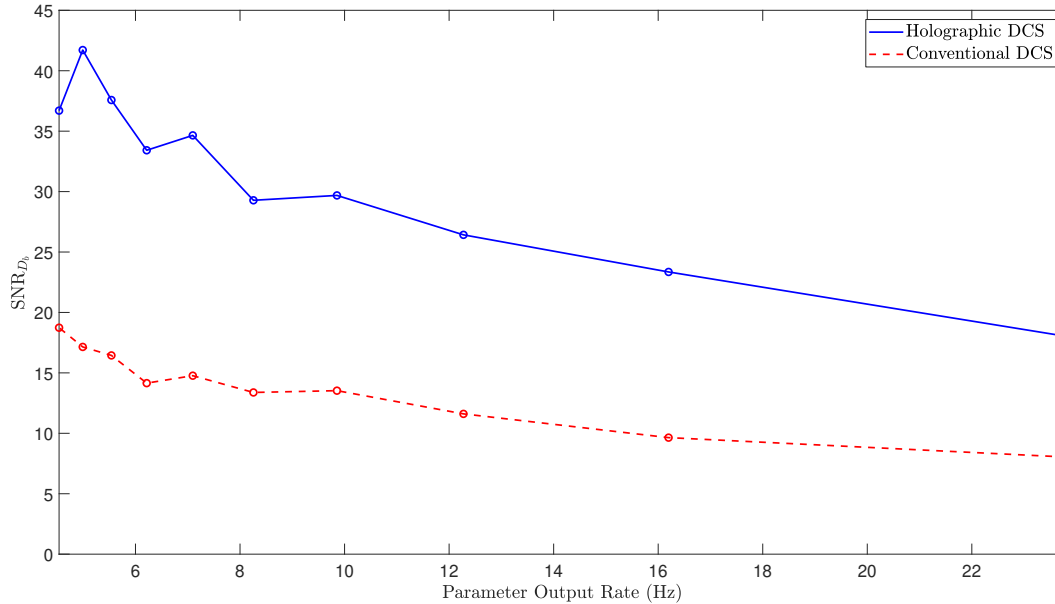


Figure 2. Evaluation of  $\text{SNR}_{D_b}$  performance over a range of parameter output rates for both conventional DCS and holographic DCS.

We define the SNR of a  $D_b$  measurement to be the mean  $D_b$  value over  $N$  measurements, divided by the standard deviation in those measurements

$$\text{SNR}_{D_b} = \frac{\mu(D_b)}{\sigma(D_b)}. \quad (2)$$

To assess the SNR benefit conferred by our instrument under optical blackout conditions, we assessed  $\text{SNR}_{D_b}$  over a range of parameter output rates in an intralipid phantom with optical properties similar to that of brain tissue,<sup>6</sup> for  $N = 100$ . By varying the number of frequency shifts per  $D_b$  frame, as well as the number of camera exposures at each frequency shift, we can carefully control the overall parameter output rate of our instrument. This is depicted by the blue curve in Figure 2. The red dashed curve in this figure shows  $\text{SNR}_{D_b}$  values for a conventional DCS technique, obtained under equivalent parameter output rates. Our holographic DCS instrument has an improvement over conventional DCS, in terms of  $\text{SNR}_{D_b}$  performance, by a factor of  $\sim 2.5$ . However, repeating this experiment under normal ambient lighting conditions increases this  $\text{SNR}_{D_b}$  improvement factor to  $\sim 6.5$ . This confirms the relative insensitivity of the holographic DCS technique to ambient light.

The feasibility of making *in vivo* measurements with our instrument was demonstrated by acquiring forearm contact measurements. Our *in vivo* probe used an SDS of 11.3 mm and the beam was expanded in order to adhere to patient safety limits.<sup>22</sup> By using a parameter output rate of 10.8 Hz, pulsatile information could be accurately recovered (Figure 3, which also shows equivalent conventional DCS data), which we expect to contain significant frequency content at 1-2 Hz. Fourier transforms of these  $D_b$  time series are shown in Figure 4, which reveal peak content at 65 beats per minute in both cases. This was consistent with the resting heart rate of the volunteer in this study.

The SNR of a speckle detection system should scale linearly with the square root of the number of speckles detected.<sup>23</sup> We therefore sought to verify this for the raw  $S_1$  values produced by our instrument. Here we define the SNR in  $S_1$  to be

$$\text{SNR}_{S_1} = \frac{\mu(S_1)}{\sigma(S_1)}, \quad (3)$$

with a sample size of  $N = 500$  values in this case. By varying the size of the reconstruction mask in the holographic demodulation process, we can effectively control the number of speckles that contribute to each  $S_1$  measurement. The resulting SNR values are plotted in Figure 5, where we expect to observe a linear fit between

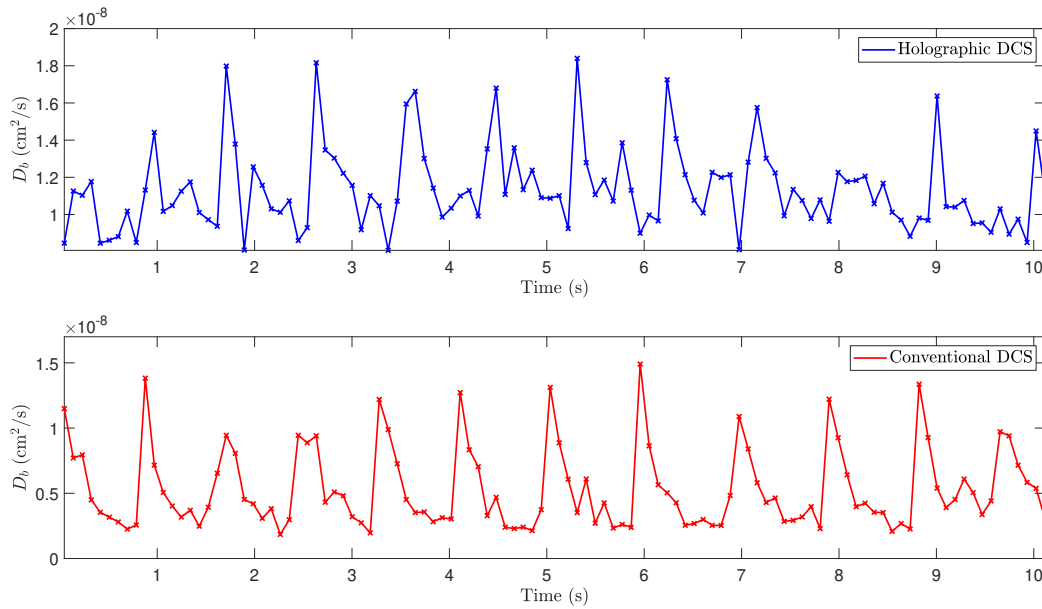


Figure 3.  $D_b$  time series for contact forearm measurements acquired at 10.8 Hz, using both conventional DCS and holographic DCS.

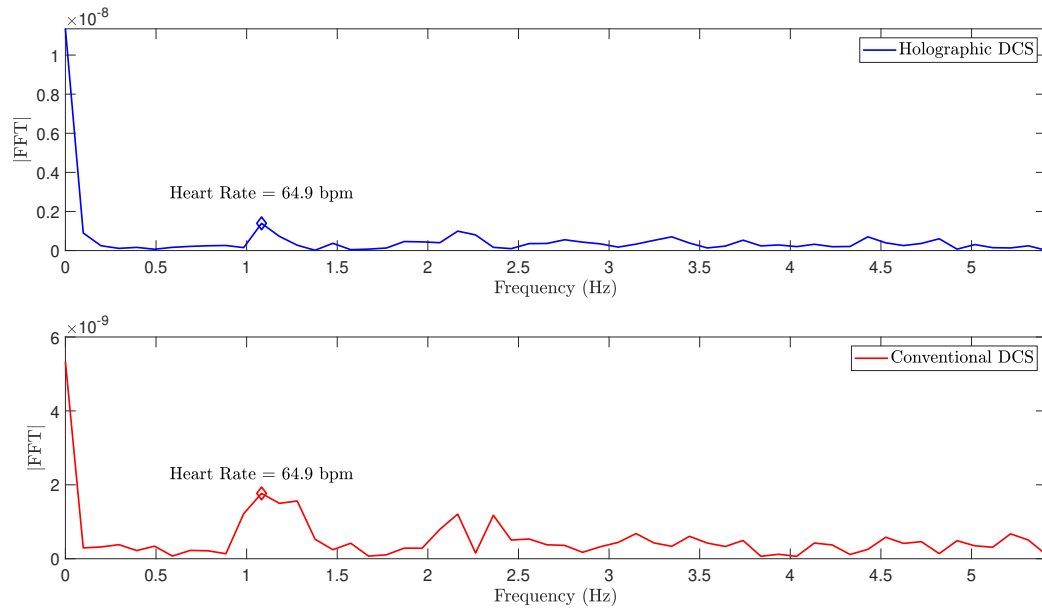


Figure 4. One-sided amplitude spectra of the  $D_b$  time series in Figure 3, acquired using a fast Fourier transform (FFT).

the SNR and square root of the number of detected modes in all 6 subplots. Instead, the SNR of  $S_1$  appears to form an asymptote towards a value of 30, which suggests another source of noise is limiting, especially at smaller detuning frequencies. We believe that this effect is in part due to variations in both the width of the measured power spectra and the drop in optical source intensity across the aperture of our holographic DCS instrument.

#### 4. CONCLUSIONS

We have shown that our holographic DCS system can measure data that is entirely equivalent to a conventional DCS system, but with a higher optical throughput and improved SNR, a decreased cost of detector, and a

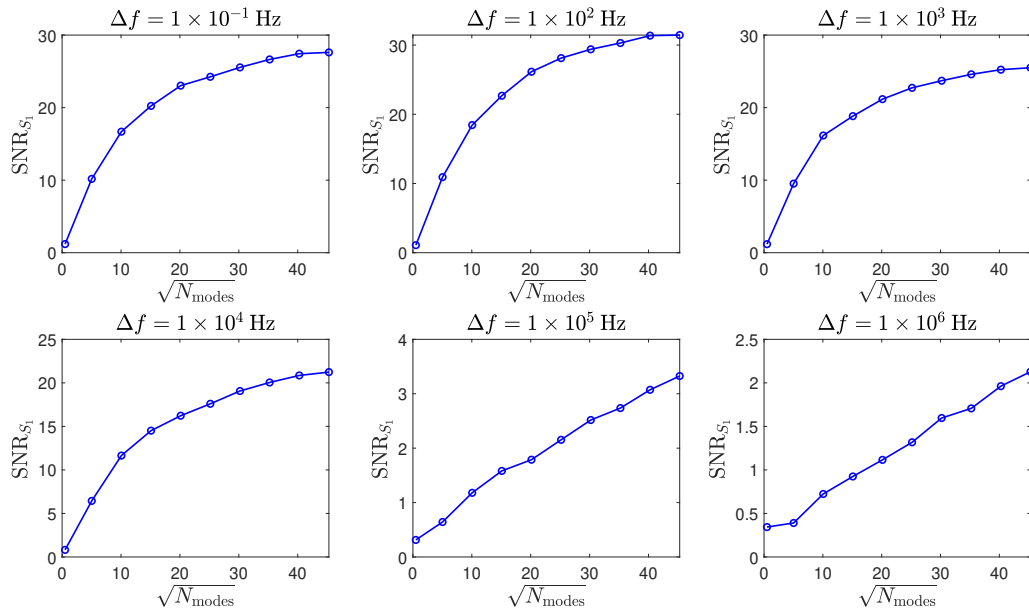


Figure 5.  $\text{SNR}_{S_1}$  does not scale linearly with the square root of the number of modes detected at smaller detuning frequencies ( $\Delta f$ ).

robustness to the effects of ambient light. By developing and validating a Brownian DCS frequency domain model, we are able to achieve optimal interpretation of the data produced by our instrument in its native domain, which is fundamentally different to conventional DCS data. These differences arise due to the alternative sampling strategies of data in the time and frequency domains, the effects of static scattering in a holographic DCS system, the nature of the noise, and broadening by the IRF, especially at high parameter output rates. These high output rates have been made possible by the design of our custom instrument with a high throughput and minimal dead-time, which enables highly parallel GPU-accelerated holographic demodulation and is thus suited to *in vivo* application.

Our future work will involve overcoming the issues encountered with SNR scaling and completing our Fourier domain DCS model with a convective flow measurement. Validation of an SNR advantage is a necessary precursor to enhancing the spatial resolution and imaging depth of our instrument using ultrasound modulation.

## ACKNOWLEDGMENTS

This work was supported by the EPSRC-funded UCL Centre for Doctoral Training in Medical Imaging (EP/L0164-78/1), the Department of Health's NIHR-funded Biomedical Research Centre at Cambridge University Hospitals, and EPSRC grant EP/N032055/1. S. Powell further acknowledges support of The Royal Academy of Engineering Fellowship RF1516\15\33.

## REFERENCES

- [1] Buckley, E. M., Parthasarathy, A. B., Grant, P. E., Yodh, A. G., and Franceschini, M. A., "Diffuse correlation spectroscopy for measurement of cerebral blood flow: future prospects," *Neurophotonics* **1**(1), 1–7 (2014).
- [2] Durduran, T., Choe, R., Baker, W. B., and Yodh, A. G., "Diffuse optics for tissue monitoring and tomography," *Reports on Progress in Physics* **73**(7) (2010).
- [3] Zhou, W., Kholiqov, O., Chong, S. P., and Srinivasan, V. J., "Highly parallel, interferometric diffusing wave spectroscopy for monitoring cerebral blood flow dynamics," *Optica* **5**(5), 518 (2018).
- [4] Markus Rudin, [*Molecular Imaging : Basic Principles and Applications in Biomedical Research*], London, Imperial College, 2nd ed. (2013).

- [5] Elson, D. S., Li, R., Dunsby, C., Eckersley, R., and Tang, M.-X., “Ultrasound-mediated optical tomography: a review of current methods,” *Interface Focus* **1**(4), 632–648 (2011).
- [6] Wang, D., Parthasarathy, A. B., Baker, W. B., Gannon, K., Kavuri, V., Ko, T., Schenkel, S., Li, Z., Li, Z., Mullen, M. T., Detre, J. A., and Yodh, A. G., “Fast blood flow monitoring in deep tissues with real-time software correlators,” *Biomedical Optics Express* **7**(3), 776 (2016).
- [7] Resink, S. G., “State-of-the art of acousto-optic sensing and imaging of turbid media,” *Journal of Biomedical Optics* **17**(4), 1–10 (2012).
- [8] Gunther, J. and Andersson-Engels, S., “Review of current methods of acousto-optical tomography for biomedical applications,” *Frontiers of Optoelectronics* **10**(3), 211–238 (2017).
- [9] Marks, F. A., Tomlinson, H. W., and Brooksby, G. W., “Comprehensive approach to breast cancer detection using light: photon localization by ultrasound modulation and tissue characterization by spectral discrimination,” *Proceedings of SPIE* **1888**(September 1993), 500–510 (1993).
- [10] Atlan, M. and Gross, M., “Spatiotemporal heterodyne detection,” *Journal of the Optical Society of America A* **24**(9), 2701–2709 (2007).
- [11] Gross, M., “Heterodyne holography with full control of both the signal and reference arms,” *Applied Optics* **55**(3), A8 (2016).
- [12] Verpillat, F., Joud, F., Atlan, M., and Gross, M., “Digital holography at shot noise level,” *IEEE/OSA Journal of Display Technology* **6**(10), 455–464 (2010).
- [13] Gross, M., Goy, P., and Al-Koussa, M., “Shot-noise detection of ultrasound-tagged photons in ultrasound-modulated optical imaging,” *Optics letters* **28**(24), 2482–4 (2003).
- [14] Bencteux, J., Pagnoux, P., Kostas, T., Bayat, S., and Atlan, M., “Holographic laser Doppler imaging of pulsatile blood flow,” *Journal of the Optical Society of America A* **31**(12) (2015).
- [15] Yu, G., Durduran, T., Zhou, C., Cheng, R., and Yodh, A. G., “Near-Infrared Diffuse Correlation Spectroscopy for Assessment of Tissue Blood Flow,” in [*Handbook of Biomedical Optics*], 195–216 (2011).
- [16] Atlan, M., Desbiolles, P., Gross, M., and Coppey-Moisan, M., “Parallel heterodyne detection of dynamic light-scattering spectra from gold nanoparticles diffusing in viscous fluids,” *Optics Letters* **35**(5), 787 (2010).
- [17] Einstein, A., “On the Motion of Small Particles Suspended in a Stationary Liquid,” *Annalen der Physik* **322**, 549–560 (1905).
- [18] Edward, J. T., “Molecular volumes and the Stokes-Einstein equation,” *Journal of Chemical Education* **47**(4), 261 (1970).
- [19] Schätzel, K., Drewel, M., and Stimac, S., “Photon correlation measurements at large lag times: Improving statistical accuracy,” *Journal of Modern Optics* **35**(4), 711–718 (1988).
- [20] Laurence, T. A., Fore, S., and Huser, T., “Fast, flexible algorithm for calculating photon correlations,” *Optics Letters* **31**(6), 829 (2006).
- [21] Kodach, V. M., Faber, D. J., van Marle, J., van Leeuwen, T. G., and Kalkman, J., “Determination of the scattering anisotropy with optical coherence tomography,” *Optics Express* **19**(7), 6131 (2011).
- [22] The British Standards Institution, “BS EN 60825-1 : 2014 - Safety of laser products,” (December) (2017).
- [23] Varma, H. M., Valdes, C. P., Kristoffersen, A. K., Culver, J. P., and Durduran, T., “Speckle contrast optical tomography: A new method for deep tissue three-dimensional tomography of blood flow,” *Biomedical Optics Express* **5**(4), 1275 (2014).